Mechanism for the Degradation of Erythromycin A and Erythromycin A 2′-Ethyl Succinate in Acidic Aqueous Solution

Abdolreza Hassanzadeh,[†] Jill Barber,[†] Gareth A. Morris,[‡] and Peter A. Gorry*[,‡]

Schools of Pharmacy and Pharmaceutical Sciences and Chemistry, University of Manchester, Oxford Road, Manchester, M13 9PL, U.K.

Received: April 19, 2007; In Final Form: July 10, 2007

A major drawback of the antibiotic erythromycin A is its extreme acid sensitivity, leading to rapid inactivation in the stomach. The accepted model for degradation in aqueous acidic solution has erythromycin A in equilibrium with erythromycin A enol ether and degrading to anhydroerythromycin A. We report a detailed kinetic study of the acidic degradation of erythromycin A and of erythromycin A 2′-ethyl succinate (the market-leading pediatric prodrug), investigating the reaction rates and degradation products via NMR. This reveals that the accepted mechanism is incorrect and that both the enol ether and the anhydride are in equilibrium with the parent erythromycin. By implication, both the anhydride and enol ether are antibacterially inactive reservoirs for the parent erythromycin. The actual degradation pathway is the slow loss of cladinose from erythromycin A (or erythromycin A 2′-ethyl succinate), which is reported here for the first time in a kinetic study. The kinetic analysis is based on global, nonlinear, simultaneous least-squares fitting of time course concentrations for all species across multiple datasets to integrated rate expressions, to provide robust estimates of the rate constants.

Introduction

Erythromycin A (EA, **1**) is an important macrolide antibiotic used extensively in the treatment of humans and animals. In particular, it is often used in the treatment of penicillin-sensitive patients.[1] Although it is safe and effective, erythromycin A is not without its problems, principally its extreme acid sensitivity,[2] vile taste,[3,4] and severe gastric disturbance.[4] These problems have led to the development of taste-free and somewhat acid-resistant prodrug esters such as erythromycin A 2′-ethyl succinate (EAES, **4**).[5,6] These have little intrinsic antibacterial activity and require hydrolysis to create the parent drug.[7,8] EAES is currently the market-leading pediatric erythromycin.

It has long been known that EA converts rapidly under acid conditions to two inactive metabolites: erythromycin A enol ether (EAEE, **2**) and anhydroerythromycin A (AEA, **3**), destroying the antibiotic activity. Indeed, it is this rapid inactivation that necessitates the administration of large doses of erythromycin A to achieve antimicrobial action. This, in turn, can lead to further problems since EA and its metabolites are processed by the same cytochrome P450 enzymes as a number of other drugs. For example, P450 saturation by erythromycin can lead to overdose of theophylline.[9]

Although the literature on the stability of EA in acidic aqueous solution is extensive, there are comparatively few kinetic studies of the reactions involved. The first systematic study was carried out by Atkins and co-workers,[10] using (mainly) spectrophotometric methods to follow the EAEE concentration. They investigated the effects of pH, buffer concentration, and temperature on the degradation of EA and found that the degradation was subject to both general and specific acid catalysis. They proposed a simple two-step mechanism based on pseudo-first-order kinetics, Model I shown in Table 1, with sequential conversion of the parent drug (EA) to the enol ether and then to AEA. However, a weakness of the analysis was the use of the "initial rate" method[11] to obtain the rate constants. This is a dangerous methodology unless the mechanism is well-established and the validity of the approximation can be determined. Generally, complex schemes of first-order reactions involving reversible reactions will be poorly treated by this approach. Where the reaction mechanism is uncertain, the only robust procedure is to fit concentration-time data simultaneously for all species to integrated rate equations for the model under consideration.

Soon after this mechanism was published, Hoogmartens et al.[12,13] proposed a new mechanism, Model II in Table 1. This was markedly different in that the enol ether (EAEE) was in equilibrium with EA and the anhydroerythromycin (AEA) results from reaction of EA not EAEE. Experimentally, high-performance liquid chromatography and UV detection were used to monitor the concentrations of EA, EAEE, and AEA for two datasets starting from either 100% EA or 100% EAEE. These datasets were then fitted to numerically integrated rate expressions using a nonlinear regression program. The single most important observation was that incubation of the enol ether under mildly acidic condition (phosphate buffer pH 3.86) resulted in the production of EA and AEA. This immediately proved that the EA → EAEE step must be reversible, but still left open the question as to whether AEA arose from the reaction of EAEE or EA. Four alternative kinetic models were tested against the EA, EAEE and AEA data. The only model found capable of describing all the observed concentration-time profiles was Model II, although even here agreement was not perfect and the two datasets show some inconsistency.

Model II essentially became the accepted kinetic model for aqueous acid degradation of erythromycin, but with the later

* To whom correspondence should be addressed. E-mail: peter.gorry@manchester.ac.uk.
[†] School of Pharmacy and Pharmaceutical Sciences.
[‡] School of Chemistry.

10.1021/jp073030y CCC: $37.00
Published on Web 09/19/2007

TABLE 1: Reaction Schemes for Degradation of Erythromycin A in Aqueous Acidic Solution[a]

Model	Scheme	Date	Ref
I	$\mathrm{EA} \xrightarrow{k_a} \mathrm{EAEE} \xrightarrow{k_b} \mathrm{AEA}$	1986	Atkins et al.[10]
II	$\mathrm{EAEE} \underset{k_2}{\overset{k_1}{\rightleftharpoons}} \mathrm{EA} \xrightarrow{k_3} \mathrm{AEA}$	1989	Hoogmartens et al.[12,13]
III	$\mathrm{EAEE} \underset{k_2}{\overset{k_1}{\rightleftharpoons}} \mathrm{EA} \underset{k_4}{\overset{k_3}{\rightleftharpoons}} \mathrm{AEA}$	2006	Barber et al.[19]
IV	$\mathrm{EAEE} \underset{k_2}{\overset{k_1}{\rightleftharpoons}} \mathrm{EA} \underset{k_4}{\overset{k_3}{\rightleftharpoons}} \mathrm{AEA}$; $\mathrm{EA} \xrightarrow{k_5} \mathrm{CLAD}$		This work

[a] Model III is not strictly a degradation model because there is no final degradation product.

addition of a rapid equilibrium between the major (keto) form of EA (**1a**) and a (minor) hemiacetal form (**1b**). In fact, both 6,9- and 12,9-cyclized hemiacetal configurations are possible, but it has been shown that the 12,9-hemiacetal is dominant in aqueous solution[14,15] with a ketone/hemiacetal ratio of 5:2. Kinetically, the model is unchanged but EA now stands for the total concentration of keto plus 9,12-hemiacetal forms. There is strong evidence to suggest that the AEA results from dehydration of the 9,12-hemiacetal form, following the determination that the C-9 position (the spiro carbon) in AEA has *R* stereochemistry. Formation of AEA from a 6,9-cyclized oxonium ion would lead to 9*S* stereochemistry, but a 12,9-cyclized oxonium ion would lead to 9*R*.[16] In contrast, the enol ether is found to be 6,9-cyclized,[17] suggesting that it results from reaction of the keto form.

More recently Kim et al.[18] have investigated the pH dependence of the aqueous acidic and basic degradation of EA adopting model II. Concentrations of EA were determined by reverse phase HPLC and electrochemical detection. Their analysis explicitly includes the EA(keto) ⇔ EA(hemiacetal) equilibrium, but unfortunately assigns the hemiacetal to the 6,9-cyclized form based on earlier studies from the 1970s. They also report the hemiacetal to be the largest component at approximately 80%. On this basis, they propose that the 6,9-hemiacetal is the precursor to both EAEE and AEA production. The rate constant for degradation is obtained by fitting the EA curve to a single exponential and, by assuming a large excess of hemiacetal and ignoring the enol ether pathway, they simplify the differential rate equations describing Model II using an initial rate approach to develop an approximate model of the pH dependence. Unfortunately, the analysis has a number of simplifications that make it difficult to judge the accuracy of the conclusions. Fitting the EA degradation to a single exponential is inconsistent with model II. It is possible to obtain analytic solutions to the differential equations of model II by the Laplace transform method, as shown in the Supporting Information. The resultant expression for the concentration of EA is

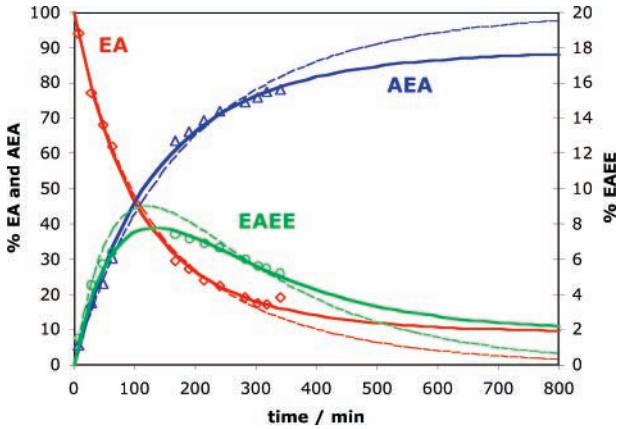

Figure 1. Fits to Model II (dashed) and Model III (solid) to the data of Hoogmartens.[12,13] Note the expanded scale (right axis) for the EAEE component.

$$[EA]_t = \frac{(k_p - k_c)[EA]_0}{2k_p}\{e^{-1/2(k_p - k_t)t}\} + \frac{(k_p + k_c)[EA]_0}{2k_p}\{e^{-1/2(k_p + k_t)t}\} \quad (1)$$

where $k_t = k_1 + k_2 + k_3$, $k_c = k_1 - k_2 + k_3$, and $k_p = \sqrt{k_t^2 - 4k_2k_3}$

We see that the $[EA]_t$ curve for model II is biexponential and involves all three rate constants in a complex way; fitting to a single exponential is not justified. The use of the 6,9-hemiacetal as a common precursor to AEEE and AEA is also in severe doubt given the stereochemistry argument above, and invalidates the derivation given in eqs 1−5 of the paper.[18] The assertion that the hemiacetal is the major component of EA is at odds with NMR results,[14,15] and casts doubt on the approximations applied. It is likely that the broad conclusions of Kim et al. are correct with regard to pH stability, but the accuracy of their numerical values is at best unclear, especially because we now show that Model II is itself incorrect.

Finally, Barber et al. have recently reported a detailed kinetic study of erythromycins A and B and their 2′-ethyl succinates over a range of acid pH.[19] In this study, concentrations of EA, EAEE, and AEA were measured by NMR, and the concentration profiles were fitted to the integrated rate expressions for the kinetic model under consideration. Rate constants were found by global nonlinear least-squares optimization against the time course data for multiple species across multiple datasets. Initially, the analysis was based on Model II, but it was found that at low pH long time course data were poorly described by this model. In particular, it was found that at long times the proportion of AEA did not tend to 100% and EA and EAEE to 0%, as required by Model II. It was found necessary to adopt a double equilibrium model, Model III in Table 1, in which AEA was formed reversibly from EA. In this model both EAEE and AEA are inactive reservoirs for EA, with pH-dependent equilibrium concentrations. We stress this was adopted as a stopgap solution to finding the best estimates of the rate constant for loss of EA. Model III is not a degradation model and immediately raises the question: what then is the actual degradation pathway for EA? It is this question that led to the study reported here, where we establish a new mechanism in

TABLE 2: Fitted Parameters for the Hoogmartens EA Dataset[12a]

	model	SS	$k_1/10^{-3}$ min^{-1}	$k_2/10^{-2}$ min^{-1}	$k_3/10^{-3}$ min^{-1}	$k_4/10^{-3}$ min^{-1}
original analysis	II	−	2.1 ± 0.39	1.0 ± 0.22	6.2 ± 0.11	−
this paper	II	0.0134	2.16 ± 0.35	1.0 ± 0.20	6.2 ± 0.10	−
this paper	III	0.0056	1.7 ± 0.23	0.83 ± 0.14	7.0 ± 0.16	0.72 ± 0.11

[a] The quoted error limits are half those of eq 6 for consistency with the original paper.

which the actual degradation pathway is the slow loss of cladinose from EA, Model IV in Table 1.

Experimental Section

General Procedures. All chemicals were purchased from Sigma Aldrich unless otherwise stated. ^{1}H NMR spectra were acquired using a Varian Unity 500 spectrometer operating at 500 MHz or a Bruker AVANCE 300 specrometer operating at 300 MHz. Electrospray-ionization mass spectra (ESI-MS) were acquired on a Micromass Platform mass spectrometer, and the data were analyzed using the program PLATFORM with a Masslynx data system. Ten microliters of the sample were injected using a Hewlett-Packard auto-sampler, and the machine was operated at a cone voltage of 30 eV at 80 °C. For identification purposes, all samples (0.2 mg) were prepared in acetonitrile (1 mL). Water was used as the solvent for running the samples.

Chemical syntheses. Compounds **1** and **4** are available commercially.

Synthesis of Erythromycin A Enol Ether (2). Erythromycin A enol ether was prepared by a published procedure,[17] and its structure was confirmed by NMR spectroscopy. Yield 68%, mp 133−138 °C (lit. 135−140 °C).[17]

Synthesis of Erythromycin A Enol Ether 2′-Ethyl Succinate (5). Erythromycin A enol ether 2′-ethyl succinate was prepared as previously described,[20] and its structure was confirmed by NMR spectroscopy. Yield 72%, mp 111−113 °C (lit. 114−116 °C).[20]

Synthesis of Anhydroerythromycin A (3). Anhydroerythromycin A was prepared by a minor adaptation of the procedure used by Stephens and Conine.[21] Yield 81%, mp 140−149 °C (lit. 142−150 °C).[22]

Synthesis of Anhydroerythromycin A 2′-Ethyl Succinate (6). Anhydroerythromycin A 2′-ethyl succinate was prepared by a published procedure[19] based on a procedure for the preparation of 2′-esters of erythromycin.[23] Its structure was confirmed by NMR spectroscopy; mp 92−102 °C (from dichloromethane-hexane); *m*/*z* (Electrospray) 845 $[M + 2H]^+$, (Found: C, 60.89; H, 8.85; N, 1.52%. Calcd. for $C_{43}H_{73}NO_{15}$: C, 61.19; H, 8.72; N, 1.66%).

Acid-Catalyzed Degradation Studies. One milligram of a stock solution of **1**, **3**, **4**, or **6** in d_6-acetone (approximately 100 mg mL^{-1}) was added to deuteriated sodium phosphate buffer (0.2 M) at apparent pH 3 or 3.55 as appropriate containing 1 mM TSP as a reference standard. An array of 1D ^{1}H spectra was acquired at 37 °C. Each spectrum was recorded with a spinning sample, using 2 s of water presaturation and a recycle time of 5 s. Sixty-four scans were collected per spectrum; spectra were acquired every 5 min 20 s with a 90° pulse of width 15 μs and a spectral width of 6000 Hz. The data acquired were processed where appropriate with reference deconvolution using the Free Induction Decay Deconvolution for Lineshape Enhancement (FIDDLE) algorithm[24] for line shape correction with a typical Gaussian time constant of 0.2 s, using the TSP signal as the reference, followed by cubic spline baseline correction. (The FIDDLE algorithm compares the experimental time-domain signal of a reference with that predicted by theory, multiplying the raw experimental data by the complex ratio of the two signals to produce a corrected free induction decay). Concentrations of erythromycin and derivatives were calculated from the experimental signal integrals.

Results

Data Fitting. The data analysis utilized custom-written procedures in Mathematica 5.1 running on an Apple Macintosh G5 computer. We define a sum of squares function for the fit to a single species, *m*, in a single kinetic run

$$\mathrm{SSc}_m = \sum_{i=1}^{n_{\mathrm{data}}} [d_i^m - \mathrm{model}^m(t_i^m)]^2 \qquad (2)$$

where d_i represents the concentration of the species for this curve, and $\mathrm{model}^m(t_i)$ represents the predicted model concentration for species *m*. We then sum over all species in all datasets

$$\mathrm{SS} = \sum_{m=1}^{n_{\mathrm{curves}}} \mathrm{SSc}_m = \sum_{m=1}^{n_{\mathrm{curves}}} \sum_{i=1}^{n_{\mathrm{data}}} [d_i^m - \mathrm{model}^m(t_i^m)]^2 \qquad (3)$$

This function SS is minimized to obtain the best fit across all datasets, using the FindFit function in Mathematica. The mean square error (MSE) for the fits is given by

$$\mathrm{MSE} = \frac{1}{n_{\mathrm{p}} - n_{\mathrm{k}}} \sum_{m=1}^{n_{\mathrm{curves}}} \sum_{i=1}^{n_{\mathrm{data}}} [d_i^m - \mathrm{model}^m(t_i^m)]^2 \qquad (4)$$

where n_{p} is the total number of points and n_{k} the number of parameters being fitted.

The standard errors (SE) associated with the model parameters are estimated from the curvature matrix at the solution minimum. The curvature matrix, α, is an $n_{\mathrm{k}} \times n_{\mathrm{k}}$ matrix, the elements of which are calculated from

$$\alpha_{p,q} = \sum_{m=1}^{n_{\mathrm{curves}}} \alpha c_{p,q} = \sum_{m=1}^{n_{\mathrm{curves}}} \sum_{i=1}^{n_{\mathrm{data}}} \left(\frac{\partial \mathrm{model}^m(t_i)}{\partial k_p}\right)\left(\frac{\partial \mathrm{model}^m(t_i)}{\partial k_q}\right) \qquad (5)$$

The SE associated with a particular parameter is obtained from the MSE matrix, *V*, which is calculated from the inverse of the curvature matrix. Parameter k_i has a 95% confidence interval

$$k_i = k_{\mathrm{model}} \pm 2\sqrt{V_{i,i}} \qquad \text{where } V = \alpha^{-1}\mathrm{MSE} \qquad (6)$$

The differential rate expressions for a number of trial models (including those of Table 1) were solved analytically using Laplace transforms so as to provide explicit expressions for the derivatives of eq 5 and for gradient searching in the global optimization.

Model III and the EA⇔AEA Equilibrium. The introduction of a reversible step from AEA to EA in Model III is a significant change, because it removes AEA as the acid degradation product and gives it the same status as the enol ether: a temporary, inactive reservoir for EA. In this section, we present conclusive evidence for the EA⇔AEA equilibrium. It is instructive to revisit

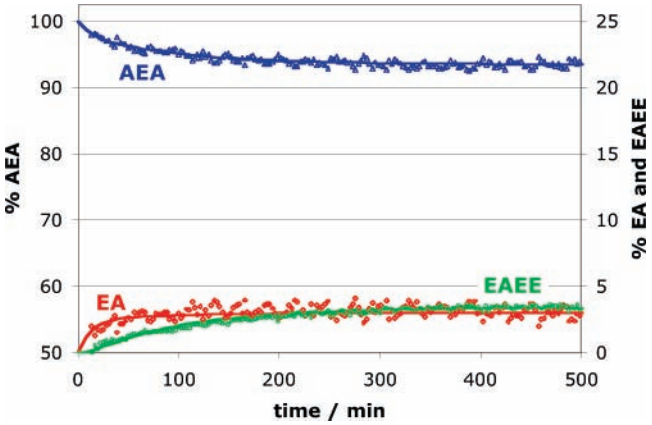

Figure 2. Equilibration of AEA to produce EA and EAEE at apparent pH = 3, T = 37 °C in deuteriated phosphate buffer (0.2 M). Note the expanded scale (right axis) for EA and EAEE. The lines are fits from Model III.

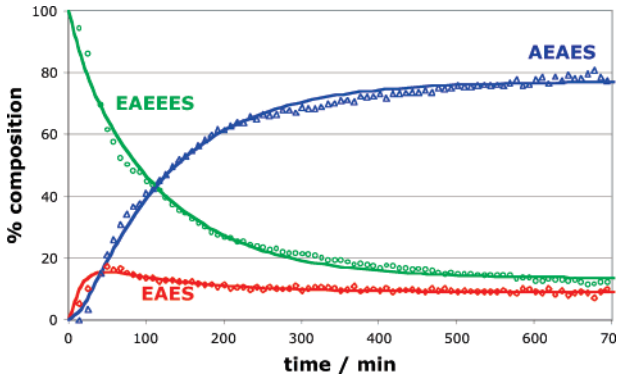

Figure 3. Equilibration of EAEEES to produce EAES and AEAES at apparent pH = 3, T = 37 °C in deuteriated phosphate buffer (0.2 M). The lines are fits from Model III.

the original Hoogmartens data[12,13] on which Model II was formulated. Although Hoogmartens et al. tested several models, they did not consider one in which the production of AEA was a reversible step, presumably because it was widely accepted that AEA was the final degradation product under aqueous acid conditions. We have reanalysed their published data against Model II and Model III. The results are shown in Figure 1 for the dataset starting from EA.

The fits for Model II are shown by dashed lines, and those for Model III by solid. We have extended the fits to longer times to show the key difference between the models: Model II moves toward 100% AEA, but Model III has equilibrium values for all three components.

The fitting statistics are given in Table 2. It is clear, even by eye, that Model III is a superior fit to the data, especially for the production and decay of EAEE. The least-squares error value *SS* (eq 3) is almost 60% smaller for Model III. It is also clear that the data do not extend to long enough times to determine unequivocally the final equilibrium concentrations.

The EAEE dataset from the Hoogmartens paper was key to demonstrating the reversibility of the EA → EAEE step. However, their analysis of this dataset proved problematic, giving a k_1 value an order of magnitude smaller than that obtained for the EA dataset. Only by constraining k_1 to the value obtained for the latter was it possible to obtain consistent values for k_2 and k_3. This illustrates a problem that arises if different kinetic parameters are sensitive to different datasets and only single datasets can be fitted at a time. For completeness, the Supporting Information includes the globally fitted rate constants

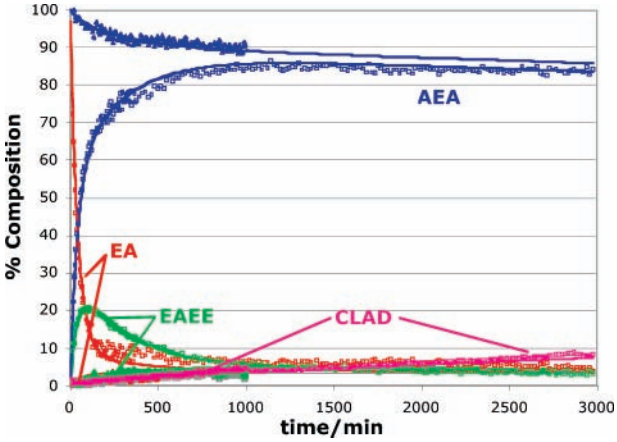

Figure 4. Acid degradation of EA (triangles) AEA (squares) at apparent pH 3, T = 37 °C in deuteriated phosphate buffer (0.2 M). The lines are a global fit to Scheme 1.

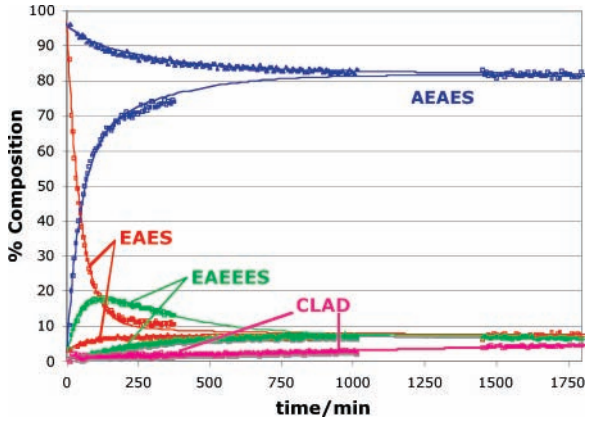

Figure 5. Acid degradation of EAES (triangles) AEAES (squares) at apparent pH = 3.55, T = 37 °C in deuteriated phosphate buffer (0.2 M). The lines are a global fit to Scheme 1.

across both datasets (eq 3). This reveals that there is some inconsistency between the datasets, with the global rate constants representing compromise values. Because of the sensitivity of the kinetics to pH (from both general and specific acid catalysis), buffer concentration, and temperature, it is experimentally challenging to obtain complete consistency.

Production of EA and AEA starting from EAEE was crucial to demonstrating the reversibility of the EA → EAEE step in the Hoogmartens study.[12] Equally, the crucial test of Model III is that EA and EAEE should be produced starting from pure AEA. Figure 2 shows previously unpublished data, taken during our earlier study,[19] where we clearly see production of EA and then EAEE from incubation of AEA, proving that the EA → AEA step is indeed reversible. The solid lines are the fit to Model III. In this earlier study, the three components were normalized to 100% throughout to maintain mass balance, disguising a small (approx 3%) loss of the three components over the time period shown. Because these experiments are carried out in deuteriated buffer, there is an additional complication from the incorporation of deuterium from the solvent D_2O at C8 by the reverse reactions EAEE → EA and the corresponding EAEEES → EAES,[19] as also observed in the earlier study of erythromycin B degradation.[2] Because the dehydration to enol ether requires the breaking of the C−H bond at C8, there is a primary kinetic isotope effect on the reverse reactions. Initially, EA rapidly forms EAES but the reverse reaction forms 8-deuterio erythromycin A (EA_D), which dehydrates more slowly than EA. Both EA and EA_D hydrolyze at the same rate

SCHEME 1: The Kinetic Model Including the Deuterium Isotope Effect. The D and H Labels Refer to the Hydrogen Isotope at Position C_8

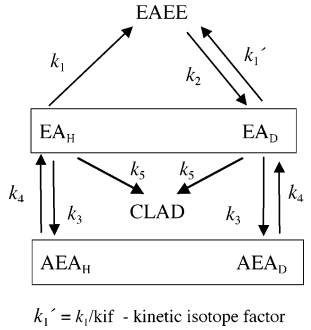

$k_1' = k_1/\text{kif}$ - kinetic isotope factor

to the AEA. This was explicitly included in the kinetic analysis of the earlier study[19] but is omitted here for the sake of simplicity; for this dataset it makes only insignificant changes to the fit shape at short time. A similar plot to Figure 2 for the anhydroerythromycin A 2′ethyl succinate (AEAES) is provided in the Supporting Information.

The data and fit to Model III for reaction starting with EA, which show the establishment of equilibrium concentrations of EAEE and AEA, are given in Figure 2 of our earlier study.[19] The corresponding data and fit from pure EAES to create EAEEES and AEAES are shown in Figure 4 of that paper. These figures are not repeated here but are included in the Supporting Information. They clearly revealed the establishment of equilibrium concentration of all three components and were the driving force for the current investigation. The fact that EAEE was in equilibrium with EA was the main revelation of the Hoogmartens paper,[13] and we show in Figure 3 that this is also true for erythromycin enol ether 2′ethyl succinate (EAEEES), but it is clear that in fact all three components, EA, EAEE, and AEA, are moving toward equilibrium values.

Model IV, the Loss of Cladinose. The previous section demonstrates unequivocally that, contrary to the long accepted belief, anhydroerythromycin is not an acid degradation product, but both EAEE and AEA are in equilibrium with EA (and so too for the 2′-ethyl succinate analogues). This leaves open the question of what the aqueous acid degradation product of EA is. An obvious candidate is the (slow) loss of the cladinose sugar (CLAD, **9**) that occurs in the acid degradation of erythromycin B, which cannot form the anhydride, to 5-*O*-desosaminyl erythronolide B. The kinetics of this degradation have been investigated previously.[2] In eryrthromycin B, the loss of the cladinose sugar is irreversible, and the kinetics are indeed of the form of Model II in which AEA is replaced by CLAD. In D_2O buffer, it is necessary to include the kinetic isotope effect at C8 in the enol ether equilibrium to fit with the short-time behavior.[2] The loss of cladinose from EA has not been reported in previous kinetic studies of the acid degradation, but there is compelling evidence that it is indeed the degradation pathway.

The earliest evidence is from the seminal 1954 study of erythromycin properties and degradation by Flynn et al.,[25] which reports the products of mild acid hydrolysis as "erythralosamine" and cladinose. Indeed, they were the first to observe and characterize the cladinose component. More relevant is the recent investigation by Volmer and Hui[26] of the aqueous acidic decomposition products of EA studied by solid-phase microextraction, liquid chromatography, and electrospray ionization tandem mass spectrometry (SPME/LC/MS). Although the authors assume that the standard Hoogmartens model (Model II) describes the degradation mechanism, the actual data reveal

TABLE 3: The Least-square Error Value, SS (eq 3), for Possible Cladinose Loss Pathways for the Data in Figure 4

cladinose loss scheme	SS
EA → CLAD	0.270
EAEE → CLAD	0.306
(EA, EAEE) → CLAD	0.310
(EA, EAEE, AEA) → CLAD	0.340
AEA → CLAD	0.358

a more complex situation. Figure 5 in ref 26 shows the SPME/LC/MS elution peaks after 24 h incubation at pH 3. The largest peak is indeed that for AEA (MH^+ *m*/*z* 716). However, a peak corresponding to EA minus cladinose (MH^+ *m*/*z* 576) and another assigned to EA minus cladinose minus H_2O (MH^+ *m*/*z* 558) are also prominent. Figure 6 of ref 21, showing the results following 24 h incubation at pH 2.2, is even more striking: the AEA elution peak is now only the third largest, the largest being EA minus cladinose with EA minus cladinose minus H_2O now second.[26] These results are not compatible with Model II, where rapid degradation to AEA should lead to this as the only product. However, they are easily explained by Model IV, where AEA can convert back to EA, which is undergoing slow degradation to cladinose and the erythronolide (**7**). The identity of the second peak, assigned to EA minus cladinose minus H_2O, is uncertain. Both EAEE and AEA result from the loss of water from EA, thus the mass peak MH^+ *m*/*z* 558 could be AEA minus cladinose or EAEE minus cladinose and Volmer and Hui do not assign this peak to a specific structure.[26] For this reason, we identify cladinose as the reaction product in Model IV, leaving open the possibility that the other moiety is erythronolide A and/or erythronolide A with simultaneous or sequential water loss.

We have carried out two sets of long time course measurements by NMR of the concentrations of EA, EAEE, AEA, and CLAD, starting from either EA or AEA at apparent pH 3.0 and 37 °C. The EA data were monitored continuously for 50 h and the AEA data for 17 h, with the results shown in Figure 4. These are the first measurement of the cladinose product in a kinetic study of the acid degradation of EA. The fits to the datasets individually are provided in the Supporting Information.

As stated earlier, the use of D_2O as the solvent complicates the kinetic scheme, and it is necessary to include the primary kinetic isotope effect for the incorporation of deuterium at the C8 position to obtain optimum fits the to data at short times.[2,19] Essentially, this initially has two linked Model IV schemes in parallel as shown in Scheme 1. However, rapid exchange means that the EA quickly converts to 8-deuterioerythromycin A, and the scheme quickly reduces to the form of a single Model IV again. For completeness, we have included this effect in the fits shown in Figure 4.

The question of the cladinose decomposition step still needs consideration. In principle, the cladinose can derive from one, some, or all of the EA, EAEE, and AEA components, because all possess the cladinose unit. We have carried out extensive modeling of the datasets in Figure 4 to investigate this step. In particular, we have performed global nonlinear fits to all four species (EA, EAEE, AEA, CLAD) across both datasets simultaneously (eq 3) for a number of models. The requirement for a single set of rate constants to fit all eight curves is a severe test of the kinetic scheme. A major difficulty is that the cladinose concentration only reaches 10% even at the longest times observed, so it has relatively small effects on the curves for the other species. Second, the establishment of Model III "equilibrium" concentrations is much faster than cladinose loss. Once these equilibrium values are reached it is impossible to distinguish between models for cladinose production. Thus, it

SCHEME 2: Acid Degradation of Erythromycin A and Erythromycin A 2′-Ethyl Succinate

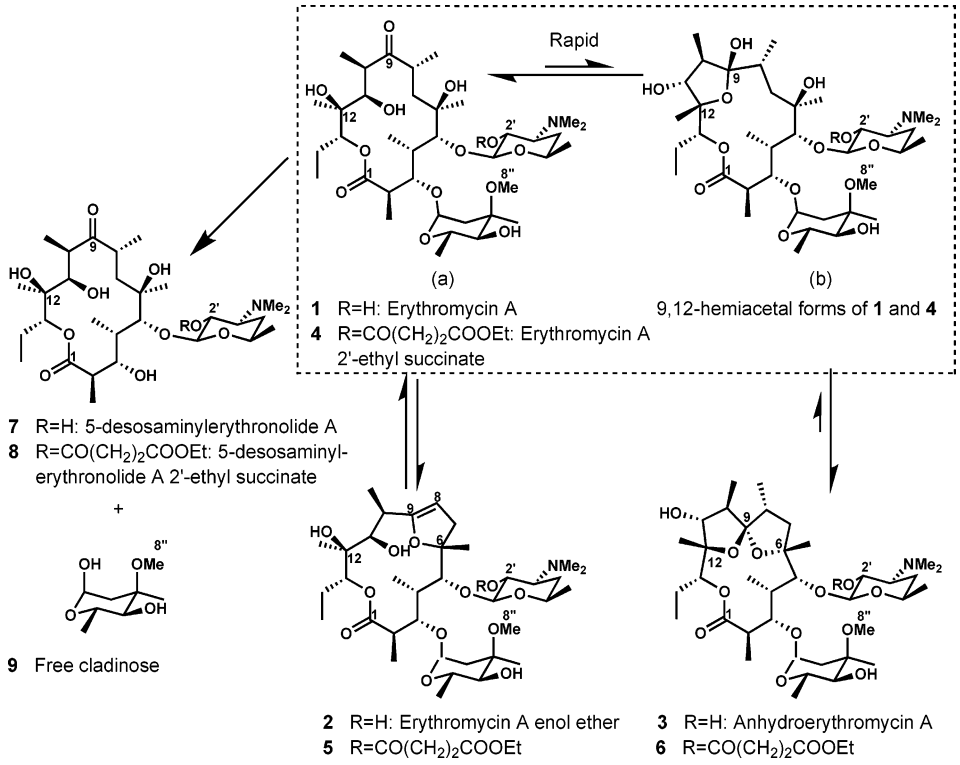

TABLE 4: Acid Degradation Rate Constants and Kinetic Isotope Factor for EA/AEA and EAES/AEAES Datasets at 37 °C in Deuteriated Phosphate Buffer (0.2 M)

dataset	pH	$k_1/10^{-3}\,\mathrm{min}^{-1}$	$k_2/10^{-3}\,\mathrm{min}^{-1}$	$k_3/10^{-2}\,\mathrm{min}^{-1}$	$k_4/10^{-4}\,\mathrm{min}^{-1}$	$k_5/10^{-4}\,\mathrm{min}^{-1}$	kif
EA/AEA	3.0	6.4 ± 0.3	4.3 ± 0.4	1.45 ± 0.02	6.9 ± 0.2	4.8 ± 0.2	1.6 ± 0.2
EAES/AEAES	3.55	4.9 ± 0.1	3.9 ± 0.2	1.34 ± 0.01	1.29 ± 0.02	2.36 ± 0.02	2.3 ± 0.2

is largely the shorter time behavior of the EA, EAEE, and AEA curves that is sensitive to the cladinose loss model. The results are given in Table 3. The SS values have three components: the inherent scatter in the data itself, residual inconsistency between datasets (e.g., from small differences in sample temperature or pH), and the goodness of fit of the model to the data. Only the last of these will produce a reduction in SS for improved models. The SS value for Model III behavior alone (no cladinose loss) is 0.655. Not surprisingly any model that includes cladinose loss is a significant improvement. Because the SS values come from over 2000 datapoints, the decreases shown are real and significant.

The best fit is from EA alone producing cladinose. The poorest fit (largest SS) is produced by a model in which cladinose is produced from AEA alone. Such a model is incapable of reproducing the AEA and cladinose time course data across both datasets. The next worst fit is one in which all three species (EA, EAEE, and AEA) degrade equally by loss of cladinose. Both of these models produce visibly poorer fits than the best model. These observations rule out a cladinose step involving AEA. The possibility of cladinose arising from EAEE is more problematic. We have investigated a number of goodness of fit criteria such as the behavior of the residuals, R^2 and the Akaike Information Criterion. Unfortunately, when fitting across multiple datasets, there are really nine measures of each, a global one and one for each concentration curve. All global values produce the same model order as Table 3. The individual curve values show more variability and are sensitive to small systematic discrepancies between datasets. On the basis of the fit statistics and the results of Volmer and Hui,[26] we propose that EA → cladinose is the only degradation step required, although a contribution from EAEE → cladinose cannot be entirely ruled out from our measurements alone.

A similar set of measurements is shown in Figure 5 for degradation of EAES and anhydroerythromycin A 2′-ethyl succinate (AEAES) at apparent pH 3.55 and 37 °C. The EAES data were monitored continuously for 6 h, then incubated further for 18 h, and finally returned to the NMR apparatus and monitored continuously until a total of 30 h had elapsed. The AEAES data were monitored continuously for approximately 17 h. The solid lines are backfits from Scheme 1. Again, the fits to the individual datasets are provided in the supporting material.

The rate constants and kinetic isotope effect value for data in Figures 4 and 5 are given in Table 4; errors are calculated at the 95% confidence level from eq 6. It is not possible to make a direct comparison with the values in Table 2 because the rate constants are sensitive to pH, temperature, and buffer composition.[10,13 18,19] However, the EA and EAES values in Table 4 differ only in pH. The values of k_3 and k_4, the anhydride equilibrium step, for EA and EAES are of particular interest. The erythromycin → anhydride rate constant, k_3, changes by a factor of 3.2, very close to the expected factor of 3.5 from the known pH dependence of k_3 from our earlier study.[19] The reverse step, k_4, displays a much larger change of a factor of 5.4, which has a significant effect on the final equilibrium concentrations, as is readily seen in Figures 4 and 5. This suggests a real reactivity difference between EA and EAES for the reverse step. The enol ether equilibrium, k_1 and k_2, seems much less sensitive to pH, but the pH dependence may be offset by intrinsic reactivity differences between EA and EAES. The kinetic isotope effect of approximately 2 is smaller than that observed in the

erythromycin B study[2] and is consistent with the observation that early time course effects are much more evident in the erythromycin B and erythromycin B 2′-ethyl succinate datasets in our previous study.[19]

Discussion

The accepted literature model for the degradation of EA in acidic aqueous solution has been shown to be incorrect; we propose the new mechanism, shown in Scheme 2, applicable to erythromycin and erythromycin A 2′-ethyl succinate. The erythromycin A (**1**, **4**) is in rapid equilibrium between its keto form (**1a**, **4a**) and the 9,12-hemiacetal form (**1b**, **4b**) with the keto form dominant. The anhydrides (**3**, **6**) arise from (reversible) dehydration of the 9,12-hemiacetal (**1b**, **4b**) to produce *R* stereochemistry at the C-9 position (the spiro carbon). The erythromycin A enol ethers (**2**, **5**) are found to be 6,9-cyclized,[17] suggesting they are produced from reaction of the keto form (**1a**, **4a**). Finally, the acid degradation pathway is the production of the erythronolide A (**7**, **8**) and free cladinose (**9**). It is not known which form of the EA leads to the cladinose.

It is obvious from earlier work and from Figures 4 and 5 and Table 4 that the rate constants in the double equilibrium of Model IV are sensitive to pH, buffer, and temperature. There are also probably reactivity differences between erythromycin A and the 2′-ethyl succinate ester. Although it would be a major undertaking, it is clear that a reinvestigation of the pH, buffer, and temperature dependence of the reaction kinetics, in which all rate constants are obtained by global fitting to integrated rate equations over multiple datasets, is now needed to gain a complete understanding of the acid degradation process for this important class of macrolide antibiotics.

In an earlier work,[20] we demonstrated the possibility of using erythromycin B enol ethers, such as erythromycin B enol ether 2′-ethyl succinate, as proprodrugs of erythromycin B. At acidic pH, under conditions resembling the stomach, erythromycin B enol ethers are rapidly hydrolyzed to erythromycin B derivatives. The enol ether esters are very poorly soluble at neutral pH and very resistant to ester hydrolysis; as a consequence, they are expected to be completely taste-free and therefore much more acceptable to children than current pediatric erythromycins. For EA, this approach to taste-free prodrugs is more difficult because k_1 (the rate constant for formation of enol ether from the corresponding erythromycin) is greater than k_2 (the rate constant for the reverse reaction) both for EA itself and for simple esters such as EAES. The differences between k_1 and k_2 are small, however, and we anticipate that the synthesis of erythromycin A enol ethers that convert to erythromycins in the body will prove possible. More speculatively, we propose the possibility of exploiting the equilibrium between EA and AEA. Erythromycins are often used in the long-term treatment of deep-seated infections, such as tuberculosis. Four times daily dosing over several months is often impractical. Anhydroerythromycin A is, as we have shown here, stable to degradation by loss of cladinose, and might form the basis of an erythromycin slow-release system.

Acknowledgment. A.H. thanks the Ministry of Health and Medical Education of Iran for a fellowship. This work was supported in part by EPSRC grant GR/590751.

Supporting Information Available: Laplace transform solutions to Model II. Global fits to Model II and Model III for Hoogmartens' EA and EAEE datasets.[12] Model III fits to our EA and EAES datasets.[19] Separated versions of Figures 5 and 6 for greater clarity. This material is available free of charge via the Internet at http://pubs.acs.org.

References and Notes

(1) Gregory, D.; Zeleznik, D.; Harnisch, J. P.; Counts, G. W. Activity of penicillin, erythromycin and cephalosporins against isolates of *Corynebacterium diphtheriae* from cutaneous lesions. *J. Antimicrob. Chemother*. **1979**, *5*, 479−81.

(2) Mordi, M. N.; Pelta, M. D.; Boote, V; Morris, G. A.; Barber, J. Acid-catalyzed degradation of clarithromycin and erythromycin B: a comparative study using NMR spectroscopy. *J. Med. Chem.* **2000**, *43*, 467−474.

(3) Graham, E. M. Erythromycin. *Obstet. Gynecol. Clin. North Am.* **1992**, *19*, 539−549.

(4) Barber, J.; Mordi, M. N. Erythromycin B, and derivatives thereof, as antibiotic agents for the treatment of microbial infections. *PCT Int. Appl*. **2000**, 45.

(5) Tsuji, K.; Goetz, J. F. Elevated column temperature for the high-performance liquid chromatographic determination of erythromycin and erythromycin ethyl succinate. *J. Chromatogr*. **1978**, *157*, 185−196.

(6) Kirst, H. A. (1993) Semi-synthetic derivatives of erythromycin. *Prog. Med. Chem.* **1993**, *30*, 57−87.

(7) Sinkula, A. A. Chemical modification of erythromycin: synthesis and preliminary bioactivity of selected amides and esters. *J. Pharm. Sci*. **1974**, *63*, 842−848.

(8) Tardrew, P. L.; Mao, J. C. H.; Kenney, D. Antibacterial activity of 2′-esters of erythromycin. *Appl. Microbiol.* **1969**, *18* (2), 159−65.

(9) Stupans, I.; Sansom, L. N. The inhibition of drug oxidation by anhydroerythromycin, an acid degradation product of erythromycin, *Biochem. Pharmacol*. **1991**, *42*, 2085−2890.

(10) Atkins, P. J.; Herbert, T.O.; Jones, N. B. Kinetic studies on the decomposition of erythromycin A in aqueous acidic and neutral buffers. *Int. J. Pharm.* **1986**, *30*, 199−207.

(11) Connors K. A. The study of reaction kinetics. *J. Parent. Sci. Technol.* **1981**, *35*, 286−208.

(12) Vinckier, C.; Hauchecorne, R.; Cachet, Th.; Van den Mooter, G.; Hoogmartens, J. A new mechanism for the decomposition of erythromycin A in acidic aqueous solution. *Int. J. Pharm.* **1989**, *55*, 67−76.

(13) Cachet, Th.; Van den Mooter, G.; Hauchecorne, R.; Vinckier, C.; Hoogmartens, J. Decomposition kinetics of erythromycin A in acidic aqueous solutions. *Int. J. Pharm*., **1989**, *55*, 59−65.

(14) Barber, J.; Gyi, J. I.; Morris, G. A.; Pye, D. A.; Sutherland, J. K. Isomerization of erythromycin A in deuterium oxide and [$^2H_6$] dimethyl sulphoxide solutions: a ^1H and ^{13}C NMR study. *J. Chem. Soc., Chem. Commun.* **1990**, 1040−1041.

(15) Barber, J.; Gyi, J. I.; Lian, L.; Morris, G. A.; Pye, D. A.; Sutherland, J. K. The structure of erythromycin A in [$^2H_6$] DMSO and buffered D_2O: full assignments of the ^1H and ^{13}C NMR spectra. *J. Chem. Soc., Perkin. Trans.* **1991**, *2*, 1489−1494.

(16) Hassanzadeh, A; Helliwell, M.; Barber, J. Determination of the stereochemistry of anhydroerythromycin A, the principal degradation product of the antibiotic erythromycin A. *Org. Biomol. Chem.* **2006**, *4*, 1014−1019.

(17) Alam, P; Buxton, P. C.; Parkinson, J. A.; Barber, J. Structural studies on erythromycin A enol ether: full assignments of the ^1H and ^{13}C NMR spectra. *J. Chem. Soc., Perkin. Trans.* **1995**, *2*, 1163−1167.

(18) Kim, Y. K.; Heinze, T. M., Beger, R.; Pothuluri, J. V.; Ceriglia, C. E. A kinetic study on the degradation of erythromycin A in aqueous solution. *Int. J. Pharm.* **2004**, *271*, 63−76.

(19) Hassanzadeh, A; Gorry, P. A.; Morris, G. M.; Barber, J. Pediatric erythromycins: a comparison of the properties of Erythromycins A and B 2′-ethyl succinates. *J. Med. Chem.* **2006**, *49*, 6334−6342.

(20) Bhadra, P. K.; Morris, G. A.; Barber, J. Design, synthesis and evaluation of stable and taste-free erythromycin proprodrugs. *J. Med. Chem.* **2005**, *48*, 3878−3884.

(21) Stephens, V. C.; Conine J. W. Esters of erythromycin. III. Esters of low-molecular-weight aliphatic acids. *Antibiot. Ann*. **1958−1959**, 346−353.

(22) Wiley, P. F.; Gerzon, K.; Flynn, E. H.; Sigal, M. V., Jr.; Weaver, O.; Quarck, U. C.; Chauvette, R. R.; Monahan, R. Erythromycin. X. Structure of erythromycin. *J. Am. Chem. Soc*. **1957**, *79*, 6062−6070.

(23) Clark, R. K.; Varner E. L. New esters of erythromycin. *Antibiot. Chemother. (Washington, D.C.)* **1957**, *VII*, 487−489.

(24) Morris, G. A.; Barjat, H; Horne, T. J. Reference deconvolution methods. *Prog. Nucl. Magn. Reson. Spectrosc*. **1997**, *31*, 197−257.

(25) Flynn, E. H.; Sigal, M. V.; Wiley, P. F.; Gerzon, K. Erythromycin. I. Properties and Degradation Studies. *J. Am. Chem. Soc.* **1954**, *76*, 3121−3131.

(26) Volmer, D. A.; Hui, J. P. M. Study of Erythromycin A decomposition products in aqueous solution by solid-phase microextraction/liquid chromatography/mass spectrometery. *Rapid Commun. Mass Spectrom*. **1998**, *12*, 123−129.